Research Square

Preprints are preliminary reports that have not undergone peer review.
They should not be considered conclusive, used to inform clinical practice,
or referenced by the media as validated information.

Monsoon and Tropical Cyclones shape mid-latitude precipitation in East Asia during the early Eocene hothouse climate

Fanni Dóra Kelemen

kelemen@iau.uni-frankfurt.de

Goethe University Frankfurt: Goethe-Universitat Frankfurt am Main https://orcid.org/0000-0002-6118-4945

Niels Meijer

Senckenberg Biodiversity and Climate Research Centre: Senckenberg Biodiversitat und Klima Forschungszentrum

Research Article

Keywords: East Asian Monsoon, tropical cyclones, paleoclimate, early Eocene

Posted Date: November 3rd, 2026

DOI: https://doi.org/10.21203/rs.3.rs-11206418/v1

License: This work is licensed under a Creative Commons Attribution 4.0 International License.
Read Full License

Monsoon and Tropical Cyclones shape mid-latitude precipitation in East Asia during the early Eocene hothouse climate

Fanni Dóra Kelemen[1*] and Niels Meijer[2]

[1*]Institute for Atmospheric and Environmental Sciences, Goethe University Frankfurt, Altenhöferallee 1, Frankfurt am Main, 60438, Germany.

[2]Senckenberg Biodiversity and Climate Research Centre, Georg-Voigt-Straße 14-16, Frankfurt am Main, 60325, Germany.

*Corresponding author(s). E-mail(s): kelemen@iau.uni-frankfurt.de;
Contributing authors: niels.meijer@senckenberg.de;

Abstract

The Asian mid-latitudes experienced a subtropical arid belt during most of the Eocene hothouse climate. This interpretation is supported by climate model simulations, but is in contrast with new proxy reconstructions, which indicate greening during the early Eocene. Here, we investigate the discrepancy between models and proxies by analysing the atmospheric circulation in the modelled climate. We assess the contribution of monsoonal circulation, extratropical and tropical cyclones to precipitation, and investigate the sensitivity of precipitation patterns to sea surface temperature (SST) changes. We find that the precipitation in our selected target region is mainly associated with monsoonal circulation and that fewer extratropical cyclones reach the target region from west than in the pre-industrial climate. Additionally, we find tropical cyclones in the model simulation, which reach the mid-latitude target region and contribute significantly to the summer precipitation. The co-existence of an extremely warm tropical ocean and the large-scale monsoonal circulation promotes tropical cyclones to reach the continental mid-latitudes, presenting an additional pathway for moisture transport into the mid-latitudes. Our sensitivity experiments show that the precipitation in our mid-latitude continental target area is sensitive to the land-sea temperature contrast, and that lowering SST values enhance the monsoonal circulation which then transports more moisture inland. Our study thus highlights that the early Eocene climate simulation underestimates the monsoonal

circulation and precipitation across the continental interior of East Asia, which is likely connected to a discrepancy in the land sea thermal contrast.

Keywords: East Asian Monsoon, tropical cyclones, paleoclimate, early Eocene

1 Introduction

Reconstructions of early Eocene (56-47.8 Ma) East Asian hydroclimate reveal a discrepancy between precipitation proxy estimates and climate-model simulations (Meijer et al. 2024; Farnsworth et al. 2019; Thompson et al. 2025). This discrepancy provides an opportunity to investigate the atmospheric circulation governing the regional hydroclimate under high-CO_2 conditions, offering insights into climate states that lie beyond the range of present day observations. A major circulation system influencing the mid-latitude East Asian climate today is the East Asian monsoon, which interacts strongly with the mid-latitude westerlies and the associated transient disturbances.

Previous proxy compilations suggested that during the early Eocene, mid-latitude China was dominated by steppe-desert shrubs (*Ephedraceae*) and evaporites, which is interpreted as a zonal arid belt with only the coastal sites being relatively humid, and monsoonal circulation restricted to the tropics (Sun and Wang 2005; Guo et al. 2008; Xie et al. 2025; He et al. 2025; Spicer et al. 2025). This is supported by climate model simulations showing a weak or absent East Asian monsoon in the early Eocene (Zhang et al. 2012; He et al. 2025; Farnsworth et al. 2019; Tardif et al. 2020, 2023).

Nevertheless, a recent study from the Xining Basin in the continental interior of China shows the abrupt spread of forests and disappearance of evaporites during the Paleocene-Eocene Thermal Maximum (PETM) (Meijer et al. 2024). The PETM was a hyperthermal event, at the beginning of the early Eocene, caused by the abrupt release of greenhouse gases lasting 100-200 ka at 56 Ma and resulting in an additional 5-6°C global warming (McInerney and Wing 2011; Westerhold et al. 2020; Tierney et al. 2022). Paleosol proxy data from the Xining Basin suggests that summer rainfall doubled during the PETM and was therefore interpreted as an intensified East Asian monsoon existing well before the large-scale surface uplift of the Tibetan Plateau (Meijer et al. 2024). Subsequent compilations of paleobotanical data show that this greening was widespread across mid-latitude China and persisted during the hothouse conditions of the early Eocene (Thompson et al. 2025; Bondarenko and Utescher 2026). Yet, so far, climate model simulations have been unable to reproduce the increased rainfall and desert greening in this region (Meijer et al. 2024; Thompson et al. 2025; Zhang et al. 2012).

The general definition of monsoon is continuously evolving, but traditionally it means an annual reversal of prevailing surface winds and a contrast between summer precipitation and a dry winter (Wang et al. 2020). The newer concept of a global monsoon however, sees it as a global-scale solstitial mode of tropical and subtropical atmospheric circulation, driven by the annual cycle of insolation, where regional monsoon systems are localized expressions of this circulation (Wang and Ding 2008; Geen et al. 2020). Hu et al. (2023) showed that over geological timescales, the global land

monsoon domain is defined mainly by the continental configuration. Beyond paleogeography, orbital configurations and topography, especially in case of East Asia the Himalayan-Tibetan uplift, has the largest influence on regional climate differences, and on the intensity and spatial distribution of monsoonal precipitation (Farnsworth et al. 2019; Roe et al. 2016).

In tropical and subtropical Asia the oscillation of solar heating, enhanced by the different heat capacity of land and ocean results in a thermal gradient leading to a pressure gradient between the East Asian Summer Low and the oceanic Western Pacific Subtropical High (Ha et al. 2012). During late spring to summer, the monsoonal circulation induces humid air flow from the sea surfaces towards the continental interior and brings precipitation along the way. The Tibetan Plateau and the westerly jet are also playing a key role in forming an east-west oriented quasi-stationary rainfall band, the Meiyu-Baiu front across Yangtze River valley and Japan (Chen and Bordoni 2014). Thus, the present-day East Asian monsoon transports atmospheric moisture deep into the Asian continental interior. The previously mentioned Xining Basin lies at the edge of the monsoonal climate today, but records summer rainfall during the PETM as well. This suggests that a monsoonal zone similar to today or even wider already existed during the PETM.

The studies investigating the time evolution of monsoon in Asia show that the modern-like East Asian monsoon developed and intensified with the Himalayan-Tibetan uplift, and started around the Miocene (He et al. 2025; Spicer et al. 2025). Before that, in the early Eocene, climate model simulations show a weak or absent monsoon in East Asia (Abhik et al. 2026; He et al. 2025; Farnsworth et al. 2019; Tardif et al. 2020, 2023). The early Eocene therefore represents a distinctive state of the East Asian monsoon, when the Tibetan Plateau was absent or substantially less developed than today. This provides an opportunity to investigate the role of non-orographic processes, particularly land–sea thermal contrast and orbital forcing (Zhang et al. 2012), in shaping East Asian monsoonal circulation under a markedly different paleogeographic configuration. Moreover, based on temperature reconstructions, the early Eocene was the warmest period of the last 66 million years (Westerhold et al. 2020) , with CO_2 concentrations 5-6 times higher than the pre-industrial level (Hönisch et al. 2023). Thus it could provide a natural laboratory to study monsoonal circulation under hothouse conditions. Especially as the response of the East Asian monsoon to extreme greenhouse warming remains unclear, and the Coupled Model Intercomparison Project (CMIP) models tend to underestimate the East Asian monsoonal circulation (IPCC 2021).

The climate model ensemble of the Deep-Time Model Intercomparison Project (DeepMIP) was specifically aimed to reconstruct the early Eocene at various atmospheric CO_2 concentrations (Lunt et al. 2017). The models agree well with the large-scale patterns predicted by proxy data (Lunt et al. 2021), but all of these simulations show a dry continental interior in Asia in contrast to the widespread forests observed in paleobotanical data (Thompson et al. 2025). This suggests that the modelled climates do not provide sufficient moisture transport to the study region. This could result from weaker winds, reduced atmospheric moisture availability or even missing circulation patterns. Insufficient wind strength may reflect differences

in the large-scale circulation, including the strength of the monsoonal circulation and the associated land–sea thermal contrast, highlighting the potential importance of air–sea interactions and land-surface processes. Alternatively, limited moisture availability may arise from underestimation of marine evaporation, differences in convective activity or terrestrial moisture recycling. The relatively warm epicontinental proto-Paratethys Sea, which extended into western China during the early Eocene (Kaya et al. 2019), may have provided both a source of atmospheric moisture and favourable conditions for extratropical cyclonic activity (Kelemen et al. 2026). Mid-latitude cyclones associated with the westerlies could therefore have contributed to precipitation in the Asian interior, potentially reaching as far as northeastern China (Meijer et al. 2019; Xie et al. 2024). Another distinctive feature of the early Eocene climate was elevated sea surface temperatures (SST) (Lunt et al. 2021), which may have favoured enhanced tropical cyclone activity. This raises the possibility that, in addition to monsoonal and extratropical precipitation, the study region may have been influenced by tropical cyclones, including systems undergoing extratropical transition (Ma et al. 2026) under the exceptionally warm conditions of the early Eocene. Additionally, orbital variations alter seasonal insolation and can strengthen the land–sea thermal contrast, thereby enhancing the intensity of monsoonal circulation during the early Eocene (Zhang et al. 2012).

Here, we study the above described model-data mismatch in detail, by using simulations of the CESM model to understand the circulation pattern and compare simulated Mean Annual Precipitation (MAP) with regional proxy reconstructions in mid-latitude China during the PETM and early Eocene. We are focusing on the role of the land–sea thermal contrast in driving the early Eocene East Asian monsoon and also perform sensitivity experiments to assess whether modifying this contrast can enhance monsoonal circulation and precipitation in the study region.

In Section 2 , we introduce the proxy compilation, the model simulation, and the cyclone-tracking methodology. Section 3.1 describes our motivation, the proxy–model discrepancy, while Section 3.2 presents the general circulation pattern of early Eocene East Asia. In Section 3.3, we describe the results of our sensitivity experiments, and in Section 3.4, we investigate the role of extratropical and tropical cyclones in the target region's precipitation. Finally, in Section 4, we discuss and summarise our findings and present our conclusions.

2 Data and Methods

2.1 Proxy compilation

Building upon previous studies (Farnsworth et al. 2019; Thompson et al. 2025), we have compiled MAP reconstructions based on paleobotanical data and focused on the Asian mid-latitudes during the PETM and early Eocene. These reconstructions follow different methodologies and thus include different biases. Paleobotanical data can be used to reconstruct paleoclimate by using the modern-day climatic tolerances of taxa that are considered as Nearest Living Relative (NLR) of taxa identified in fossil assemblages. Underlying uncertainties include the correct identification of fossil taxa and

their NLR, the quality of the modern-day climatic tolerance data, and the assumption that these tolerances extended into the past (Hollis et al. 2019). Thompson et al. (2025) applied bioclimatic analysis to their early Eocene paleobotanical compilation by combining the NLR approach with a probability density function. This analysis statistically constrains the most likely climate for a fossil assemblage to occur. We have compiled their MAP estimates for all terrestrial basins in mid-latitude China, and excluded sites with updated age models that are not early Eocene (see Appendix). We have also excluded marine sites because these may integrate a vegetation signal from a large catchment area (Hollis et al. 2019). We have added MAP estimates from previous studies using the Co-existence Approach (CA). This approach also relies on NLR but identifies a climatic range in which the taxa could co-occur instead of applying a statistical analysis (Utescher et al. 2014). This method has been heavily criticized (Grimm and Denk 2012; Grimm et al. 2016; Grimm and Potts 2016), but remains widely used (Xie et al. 2022b,a, 2024; Su et al. 2022) and therefore we have included it in our compilation. Lastly, we have also included MAP reconstructions based on soil organic carbon δ^{13}C values from one locality, the Xining Basin. This proxy is based on the relationship observed in modern-day soils dominated by C3 vegetation showing lower δ^{13}C values in regions with higher MAP due to less water stress (Meijer et al. 2024). However, poor preservation and degradation of soil organic matter increases the δ^{13}C values and would dampen the MAP signal. These MAP reconstructions should therefore be considered as minimum estimates only (Meijer et al. 2024; Stein et al. 2021; Wynn 2007).

2.2 Climate model simulationn

The study uses simulations extended from DeepMIP simulations with the Community Earth System Model version 1.2 (CESM) in an atmosphere-only mode with horizontal resolution of 1.9° x 2.5° (latitude x longitude) with 30 hybrid sigma-pressure levels in the atmosphere. In this study, the pre-industrial and an early Eocene simulation with 6 times the pre-industrial CO_2 concentration ($6xCO_2$) were used. The aim of the extension with the additional 30 years, was to have daily or even 6 hourly temporal output from the model and to make short (6 year) sensitivity experiments possible. The atmosphere-only configuration is ideal for the sensitivity experiments as the SST and sea-ice extent is considered as boundary conditions through prescribed monthly data. The early Eocene simulation includes changes in paleogeography, vegetation, aerosols and rivers and the lack of ice sheets based on the DeepMIP experimental design (Lunt et al. 2017, 2021). The simulations were directly continued from the corresponding coupled simulations in the DeepMIP ensemble (Zhu et al. 2019; Lunt et al. 2021), thus there was no need for a spin up period. In case of the sensitivity experiments, where the SST boundary conditions were decreased and increased globally with 2 K, we accounted for 1 year as spin up, and thus had two 5 year-long timeseries for our analysis. The pre-industrial simulation together with the $1xCO_2$ simulation, have been previously analysed in Kelemen et al. (2026) to evaluate the role of paleogeography on large-scale circulation patterns. For more details on the DeepMIP simulation and the early Eocene boundary conditions, see Zhu et al. (2019) and Lunt et al. (2021).

2.3 Cyclone tracking and associated precipitation

The cyclone identifying and tracking algorithm finds cyclones as mean sea level pressure minima and connects the pressure centres in time by a nearest neighbour approach (Kelemen et al. 2015, 2026). We filter the tracks based on their genesis region and length, where only cyclones lasting longer than one day are kept. We define a focus region (30-45°N and 90-115°E) based on the proxy record compilation, and divide the cyclone tracks into four categories, according to their genesis region related to the focus region. These directions are: west (W) consisting of mid-latiude cyclones in the latitude of the westerly winds, southeast (SE) consisting of cyclones originating from the tropical western Pacific ocean, thus these can be considered tropical cyclones transitioning to the extratropics; south and southwest (SSW) also originating from low latitudes but over continental area thus these are not considered tropical cyclones, rather weak extratropical cyclones or thermal lows; north and northeast (NNE) extratropical cyclones with genesis regions over the Asian continent. We also calculated the precipitation associated with the cyclones, where we applied a cyclone centered radius mask on the 6 hourly precipitation field. After testing different distances we choose a 800 km radius, which is an intermediate radius both applicable to tropical and extratropical cyclones.

3 Results

3.1 Proxy-model discrepancy

The initial motivation for our study is the inconsistency between precipitation estimates of proxies and climate model simulations over mid-latitude East Asia during the early Eocene. On Fig. 1 the comparison of the proxy record estimates and the $6xCO_2$ early Eocene CESM simulation's precipitation distribution (box-whisker plots) is shown at the corresponding locations. The locations are arranged from west to east. The model simulation generally underestimates precipitation relative to the proxy records at most sites, whereas the agreement improves toward the coast. To understand the underlying mechanisms behind this discrepancy, the precipitation distribution and the general circulation are investigated in the region between the 30° and 45°N latitude and 90° to 115°E longitude (see rectangle on Fig. 1).

3.2 General circulation pattern in early Eocene East Asia

The monthly mean simulated precipitation in the focus region shows that the monthly distribution of precipitation is very similar in the early Eocene $6xCO_2$ simulation to the pre-industrial, but at lower amplitude. The majority of the precipitation falls in the summer half year, with a maximum in August, which is 60% lower in the early Eocene than in the pre-industrial (Fig. 2). This points toward monsoonal precipitation, rather than the influence of the westerlies, which is generally stronger during the winter months.

To better understand the sources of precipitation in the focus area, the large-scale circulation is investigated through the year. Fig. 3 shows the large-scale circulation during August and February, corresponding to opposite phases of the annual cycle.

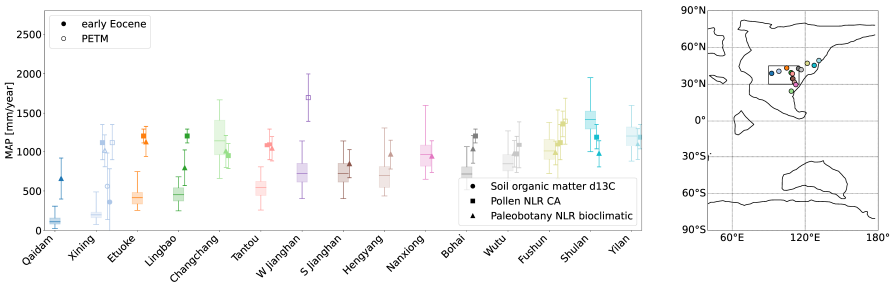


Fig. 1 Comparison of mean annual precipitation (MAP) at the proxy sites (see location on the map, ordered from west to east) from the different paleoclimatological records and from the early Eocene ($6xCO_2$) CESM1.2 simulation (box-whisker plots)

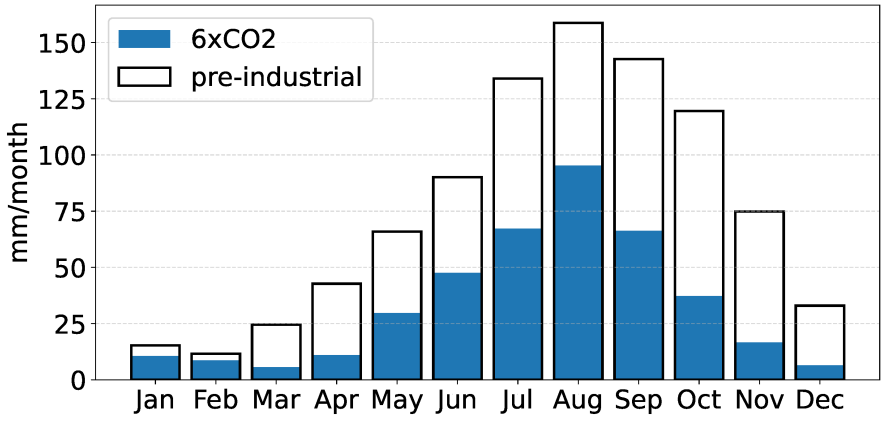


Fig. 2 Monthly mean precipitation in the focus area from the early Eocene ($6xCO_2$) CESM1.2 simulation

During winter, the focus region is in the line of the descending branch of the Hadley cell (see high pressure zone around the Tropic of Cancer, Fig. 3a), which prohibits intense precipitation formation, and the dominant wind direction is westerly (Fig. 3c). These westerlies produce some precipitation around the Paratethys region as observed by previous climate model simulations (Roe et al. 2016; Zhang et al. 2012). However, this westerly moisture is not transported far into the interior and therefore cannot explain the observed greening during the early Eocene (Meijer et al. 2024). On the other hand, during the summer months and especially during August, the Asian continent heats up stronger than the surrounding ocean and a semi-permanent thermal low, the East Asian Summer Low, develops in the middle of the continental land mass (Fig. 3b). The East Asian Summer Low is associated with large-scale cyclonic circulation with ascending air motion in the central region of the system, which promotes atmospheric lifting. Moreover, the large thermal contrast between land and ocean leads to a pressure gradient which results in the seasonally changing wind at the East Asian mid-latitudes, thus leads to monsoonal circulation (Fig. 3c and d).

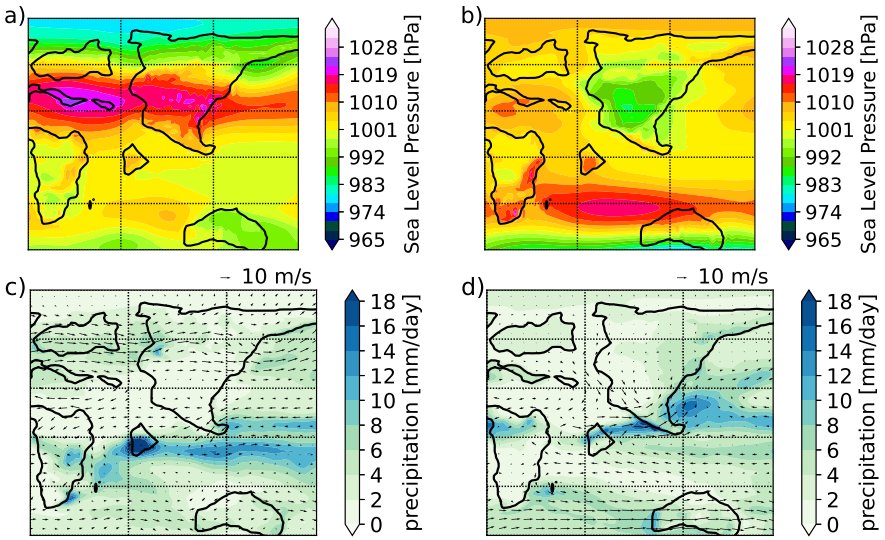


Fig. 3 Monthly mean seal level pressure (a,b), precipitation and 850 hPa wind vectors (c,d) in February (a,c) and in August (b,d) in the the early Eocene ($6xCO_2$) CESM1.2 simulation

Proxy records also suggest a summer-wet season (Meijer et al. 2024; Quan et al. 2012a), however, climate model simulations, including the one presented in this study, do not reproduce it with sufficient intensity (Meijer et al. 2024; Farnsworth et al. 2019; Zhang et al. 2012). This suggests that models underestimate the moisture transport, which is part of the monsoonal circulation and is connected to the land-see thermal contrast. An other source of uncertainty in the simulations is the poorly constrained SST of the western Pacific, due to the absence of direct proxy records from this region for the early Eocene (Hollis et al. 2019).This motivates the sensitivity experiments, which are designed to investigate how sensitive is the precipitation in the focus region, to the land and ocean thermal contrast.

3.3 Sensitivity experiments

The sensitivity experiments, with perturbed global SST boundary conditions ($\pm 2K$ SST), alter the land-sea thermal contrast. This is expected to influence the monsoonal circulation and the precipitation in the focus region. The results show that the $-2K$ SST experiment increases the mean annual precipitation at all locations, which improves the dry bias of the model, and pushes only a couple coastal locations over the proxies' range (Fig. 4).

The improvement in the $-2K$ SST experiment is due the intensification of the monsoonal circulation. The decrease in ocean temperature slightly increases the thermal contrast between the continental regions of East Asia and the western Pacific ocean, which is then detectable in the pressure fields (Fig. 5a,c and e) and in the wind fields (Fig. 5b,d and f). The stronger pull from the East Asian Summer Low, or in

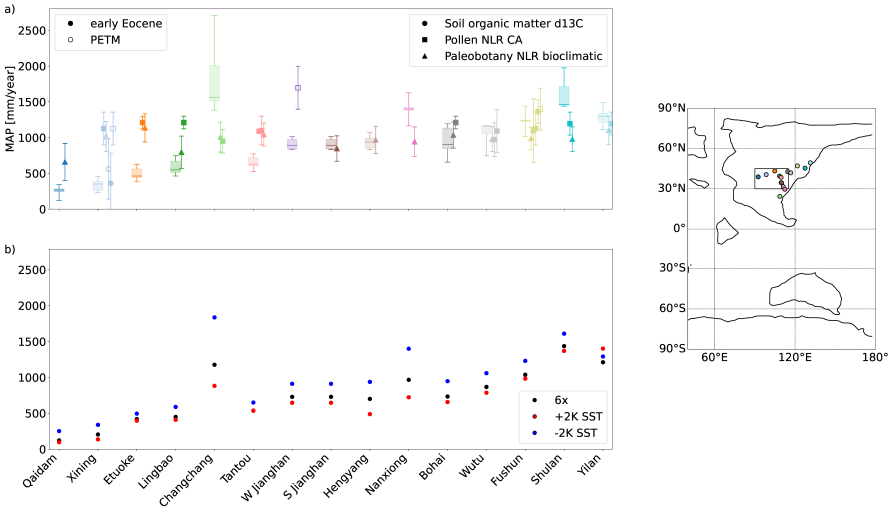


Fig. 4 Comparison of mean annual precipitation (MAP) at the proxy sites (see location on the map) from the different paleoclimatological records and from the early Eocene ($6xCO_2$) CESM1.2 sensitivity experiment with -2 K SST (box-whisker plots) (a) , and mean values from the control early Eocene ($6xCO_2$) simulation and the $+2K$ SST and $-2K$ SST sensitivity experiments (b)

other words the stronger southern wind along the eastern coast of Asia, thus increases moisture transports into the continental interior.

An additional consequence of the stronger monsoonal circulation is an increased possibility of tropical cyclones originating over the western tropical Pacific tracking across the focus region. During the five-year $-2K$ SST sensitivity experiment two such cyclones crossed the region from the southeastern direction (Fig. 6a). These cyclones, in the simulation, brought 20-40 % of the monthly total precipitation in August over the focus region's middle section (Fig. 6b), highlighting their large moisture transport capabilities.

3.4 Tropical and extratropical cyclones role in the target regions precipitation

The sensitivity studies pointed out the possibility of moisture transport into the mid-latitudes through tropical cyclones transitioning from the tropics to the extratropics. This motivated the analysis of low pressure systems crossing the focus region during the late summer months (July, August and September) in the $6xCO_2$ simulation. We divided the identified cyclone trajectories into four directions in relation to the focus region (west, southeast, southwest including south and northeast including north). The comparison between the pre-industrial and early Eocene simulations shows that westerly cyclones often deviate from the expected westerly trajectory towards south, due to the East Asian Summer Low (Fig. 7a and b). Moreover, there is a notable difference between the presence of tropical cyclones transitioning from the tropical

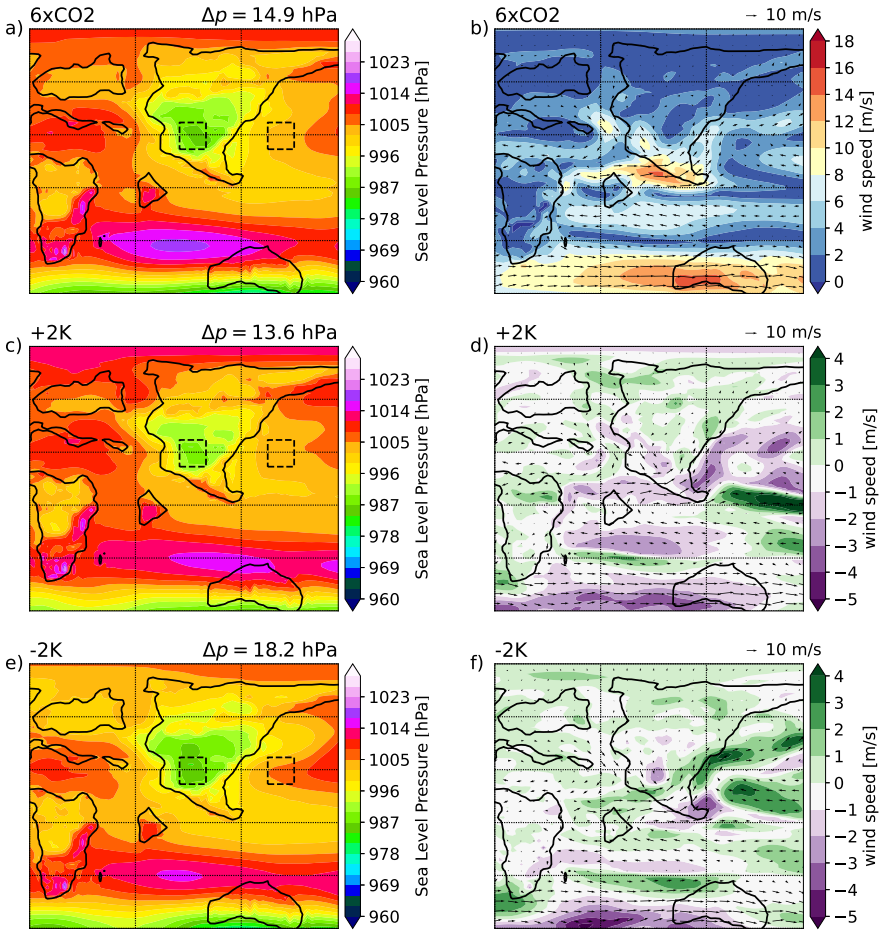


Fig. 5 Mean sea level pressure in August in the $6xCO_2$ (a) $+2K$ SST (c) and $-2K$ SST (e) simulations. The field mean of pressure is calculated in the dashed boxes and their difference is shown (upper right corner). Mean wind speed and direction at 850 hPa in August in the $6xCO_2$ simulation (b) and the sensitivity experiments' difference compared to it, $+2K$ SST (d) and $-2K$ SST (f)

Pacific Ocean to the mid-latitudes (Fig. 7c and d). Other early Eocene cyclone trajectories are also influenced by the dominant circulation of the East Asian Summer Low. Note that we only consider trajectories, which cross the focus region's borders. The annual distribution of cyclones is also different in the early Eocene simulation than in the pre-industrial (Fig. 8). The number of cyclones, crossing the target region from tropical origins increases during the summer months, probably due to the higher SST values and the influence of the East Asian Summer Low. On the other hand, the number of extratropical (westerly) cyclones crossing the focus region is substantially lower throughout the year in the early Eocene simulation, than in the pre-industrial. Globally the mid-latitude eddies' heat transport is larger in the early Eocene simulations

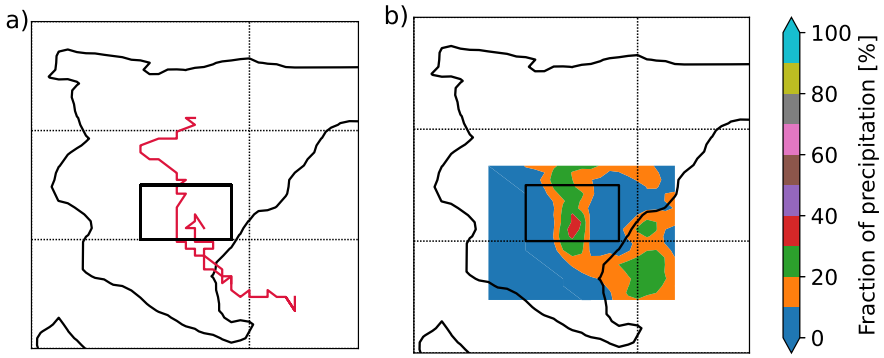


Fig. 6 Cyclone tracks which originate over the tropical Pacific ocean and cross the focus region in the -2 K SST sensitivity experiment (a) and their contribution to the precipitations of the region during August

than in the pre-industrial climate (Kelemen et al. 2023), thus one might expect more cyclones. Nevertheless, the lower meridional temperature gradient of the early Eocene, could lead to fewer cyclones, and at the same time the very warm atmosphere, which can hold more moisture, can lead to more effectively moist static energy transport.

4 Discussion and Conclusion

Early Eocene proxy records and our climate model simulations reveal a substantial proxy–model discrepancy across the mid-latitudes of East Asia, with the model exhibiting a persistent annual dry bias over the continental interior of our target region. The model simulates a precipitation maximum in August, consistent with the seasonal cycle of monsoonal precipitation. Nevertheless, the persistent dry bias suggests that the simulated monsoonal circulation and associated moisture transport are too weak to reproduce the precipitation indicated by proxy records. Other modelling studies found similar dry conditions and monsoonal precipitation only close to the coastal regions (Zhang et al. 2012; Farnsworth et al. 2019; Xie et al. 2025). This suggests that the discrepancy represents a broader challenge in simulating this circulation pattern, rather than a model-specific issue.

We investigated the atmospheric circulation during the wettest summer month (August), and compared it with the contrasting winter circulation in February. During winter, the mid-latitudes are characterised by subsidence associated with the Hadley circulation and a high pressure band. During summer, differential heating between land and ocean leads to the development of the East Asian Summer Low, which drives the monsoonal circulation, reverses the dominant wind direction, and transports moisture into the otherwise dry continental regions.The seasonal reversal of atmospheric circulation, accompanied by enhanced summer precipitation, is consistent with the general dynamical definition of a monsoon (Wang and Ding 2008; Wang et al. 2020). This seasonal reorganization can also be viewed within the framework of the global monsoon, which emphasizes the role of the annual cycle of radiative heating in driving the

seasonal migration of the global tropical atmospheric overturning and the associated convergence zone (Wang and Ding 2008; Geen et al. 2020). However, the early Eocene East Asian monsoon was weaker than its modern counterpart and exhibited a substantially different dynamical structure. In particular, the absence of a fully developed Tibetan Plateau reduced the influence of orographic forcing and its interaction with the mid-latitude westerly jet, which is important for the formation and maintenance of the modern Meiyu–Baiu frontal rainband (Geen et al. 2020). Idealised climate model simulations showed that more than half of the East Asian monsoonal precipitation is dynamically linked to the Tibetan Plateau (Son et al. 2019). Nevertheless, due to the early Eocene high atmospheric CO_2 and hothouse baseline climate, the contrasting heat capacities of land and ocean generate a seasonal thermal contrast that drives the monsoonal circulation. Thus, the early Eocene East Asian monsoonal circulation may have developed primarily through the response of the continental and oceanic surfaces to seasonal radiative forcing, rather than through the strong orographic forcing characteristic of the modern system.

Our sensitivity experiments with perturbed SSTs (± 2 K) demonstrated that the precipitation pattern is sensitive to the land–sea temperature contrast. In particular, the lower SSTs experiment showed increased summer land–sea temperature and pressure contrasts, resulting in stronger winds along the East Asian coast and an intensification of the monsoonal circulation. This enhanced circulation increased inland moisture transport in the experiment and reduced the simulated dry bias, demonstrating the importance of the land–sea thermal contrast for the representation of early Eocene monsoon precipitation.

We additionally found that part of the enhanced precipitation in the $-2K$ SST sensitivity experiment was associated with the passage of tropical cyclones. This motivated a further investigation of extratropical and tropical cyclones crossing our target region. Particularly during summer, fewer extratropical cyclones cross the target region from west in the early Eocene climate than in the pre-industrial climate. In contrast, more tropical cyclones travel northward and inland, bringing precipitation to the mid-latitudes. Precipitation associated with these cyclones show substantial interannual variability in our 5 year sensitivity experiment, and represent extreme rainfall events, in contrast with the more persistent and seasonally organized precipitation associated with the modern Meiyu–Baiu front. The influence of the East Asian Summer Low is evident across the different cyclone-track categories, particularly for tropical cyclones, which are increasingly deflected inland by the circulation associated with the East Asian Summer Low. Previous studies mostly discussed the influence of the westerlies and the East Asian monsoon in this area (Meijer et al. 2024; Xie et al. 2025; Li and Zhu 2024) thus the introduction of tropical cyclones is a new development, which is made possible through the extreme warmth of the early Eocene. Also the additional extreme precipitation which is connected to these transitioned tropical cyclones (Ma et al. 2026), can possibly contribute to the greening of the vegetation what we see in proxy records (Thompson et al. 2025).

Overall, our results indicate that in the model the monsoonal circulation is too weak and consequently it underestimates precipitation over the continental interior. A possible explanation for this discrepancy is a misrepresentation of the land–sea

thermal contrast, which may result from uncertainties in both the model simulations and proxy reconstructions. Further work integrating modelling and proxy evidence is therefore needed to better constrain this mechanism. Other aspects such as uncertainty in topography (Spicer et al. 2025; Roe et al. 2016), paleogeography (Farnsworth et al. 2026), CO_2 concentration (Licht et al. 2014) and the influence of orbital configurations (Zhang et al. 2012; Roe et al. 2016) are also possible influences in determining the regional precipitation pattern. Our results further demonstrate that tropical cyclones and other weather systems interact with the East Asian Summer Low, which can modify their trajectories and facilitate the transport of moisture and precipitation into the mid-latitudes. This novel aspect of our study is showing that the interaction between the East Asian Summer Low and tropical cyclones present an additional pathway for moisture and precipitation to reach the mid-latitudes and may therefore be important for reconciling model simulations with proxy evidence for a wetter early Eocene Asian interior.

Acknowledgements. The authors acknowledge and thank Jiang Zhu for providing the initial condition files for the CESM simulations.

Appendix A Proxy compilation

Table A1 Table of proxy compilation used in this study

site	Locality	Lat	Lon	Paleolat	Paleolon	type	age	MAP	error	Reference
Xining	Xining Basin	36.50	102.00	40.55	98.45	Soil organic matter	PETM	560	422	Meijer et al. (2024)
Xining	Xining Basin	36.50	102.00	40.55	98.45	Soil organic matter	early Eocene	360	422	Meijer et al. (2024)
Xining	Qijiachuan Fm Xining	36.50	102.00	40.55	98.45	Pollen NLR CA	PETM	1126	229	Quan et al. (2012a)
Xining	Qijiachuan Fm Xining	36.50	102.00	40.55	98.45	Paleobotany NLR	PETM	1015	208	Thompson et al. (2025)
Xining	Honggou Fm. Xining	36.50	102.00	40.55	98.45	Pollen NLR CA	early Eocene	1126	229	Quan et al. (2012a)
Fushun	Xilutian section. Fushun Basin	41.84	123.90	47.05	121.75	Pollen NLR CA	PETM	1397	291	Xie et al. (2022a)
Fushun	Xilutian section. Fushun Basin	41.84	123.90	47.05	121.75	Pollen NLR CA	early Eocene	1363	163	Xie et al. (2022a)
Fushun	Liaoning. upper Guchengzi. Fushun Basin	41.84	123.90	47.05	121.75	Pollen NLR CA	early Eocene	1126	229	Quan et al. (2012b)
Fushun	Guchengzi. Fushun Basin	41.84	123.90	47.05	121.75	Pollen NLR CA	early Eocene	1097	443	Wang et al. (2010)
Fushun	Guchengzi. Fushun Basin	41.84	123.90	47.05	121.75	Paleobotany NLR	early Eocene	988	156	Thompson et al. (2025)
W Jianghan	Longwangjing section. west Jianghan Basin	30.10	111.65	34.55	109.66	Pollen NLR CA	PETM	1696	300	Xie et al. (2022b)
Hengyang	Songmutang section. Hengyang Basin	26.96	112.61	31.55	111.20	Paleobotany NLR	early Eocene	967	189	Thompson et al. (2025)
Tantou	Tantou Basin. Tantou Fm	34.00	111.75	38.55	109.55	Pollen NLR CA	early Eocene	1087	-	Su et al. (2022)
Tantou	Tantou Basin. Tantou Fm	34.00	111.75	38.55	109.55	Pollen NLR CA	early Eocene	1097	200	Quan et al. (2012a)
Tantou	Tantou Basin	34.00	111.75	38.55	109.55	Paleobotany NLR	early Eocene	1042	160	Thompson et al. (2025)
Wutu	Wutu Coal mine	36.66	118.94	41.85	116.75	Pollen NLR CA	early Eocene	970	235	Quan et al. (2012a)
Wutu	Wutu Coal mine	36.66	118.94	41.85	116.75	Pollen NLR CA	early Eocene	1091	297	Zhang et al. (2016)
Wutu	Wutu Coal mine	36.66	118.94	41.85	116.75	Paleobotany NLR	early Eocene	977	173	Thompson et al. (2025)
Yilan	Yilan. Xinancun	46.10	129.30	49.35	131.35	Pollen NLR CA	early Eocene	1195	160	Quan et al. (2012b)
Yilan	Yilan. Xinancun	46.10	129.30	49.35	131.35	Paleobotany NLR	early Eocene	1101	201	Thompson et al. (2025)
Shulan	Shulan. Bangchuigou	44.50	126.90	45.35	127.45	Pollen NLR CA	early Eocene	1195	160	Quan et al. (2012b)
Shulan	Shulan. Bangchuigou	44.50	126.90	45.35	127.45	Paleobotany NLR	early Eocene	977	171	Thompson et al. (2025)
Qaidam	Dahonggou. Qaidam Basin	37.48	95.21	38.86	92.50	Paleobotany NLR	early Eocene	658	260	Thompson et al. (2025)
S Jianghan	ZK0303. Jianghan Basin	30.02	111.90	34.45	109.95	Paleobotany NLR	early Eocene	846	177	Thompson et al. (2025)
Changchang	CHCH1-CH3	19.60	110.40	24.35	108.65	Paleobotany NLR	early Eocene	1006	209	Thompson et al. (2025)
Changchang	CHCH1-CH3	19.60	110.40	24.35	108.65	Pollen NLR CA	early Eocene	949	164	Yao et al. (2009)
Etuoke	Etuoke Inner Mongolia	39.10	107.90	43.25	104.85	Paleobotany NLR	early Eocene	1135	197	Thompson et al. (2025)
Etuoke	Etuoke unnamed unit1 (lower)	39.10	107.90	43.25	104.85	Pollen NLR CA	early Eocene	1210	88	Quan et al. (2012a)
Bohai	Shahejie Fm Huanghua	38.30	117.30	42.75	114.55	Paleobotany NLR	early Eocene	1034	181	Thompson et al. (2025)
Bohai	Shahejie (part IV) Huanghe Bohai	38.30	117.30	42.75	114.55	Pollen NLR CA	early Eocene	1210	88	Quan et al. (2012a)
Lingbao	Lingbao Henan	34.50	110.8	39.45	108.45	Paleobotany NLR	early Eocene	794	225	Thompson et al. (2025)
Lingbao	Xiangcheng (part IV). Lingbao Basin	34.50	110.80	39.45	108.45	Pollen NLR CA	early Eocene	1210	88	Quan et al. (2012a)
Nanxiong	Nanxiong	25.10	114.30	29.65	112.35	Paleobotany NLR	early Eocene	942	206	Thompson et al. (2025)

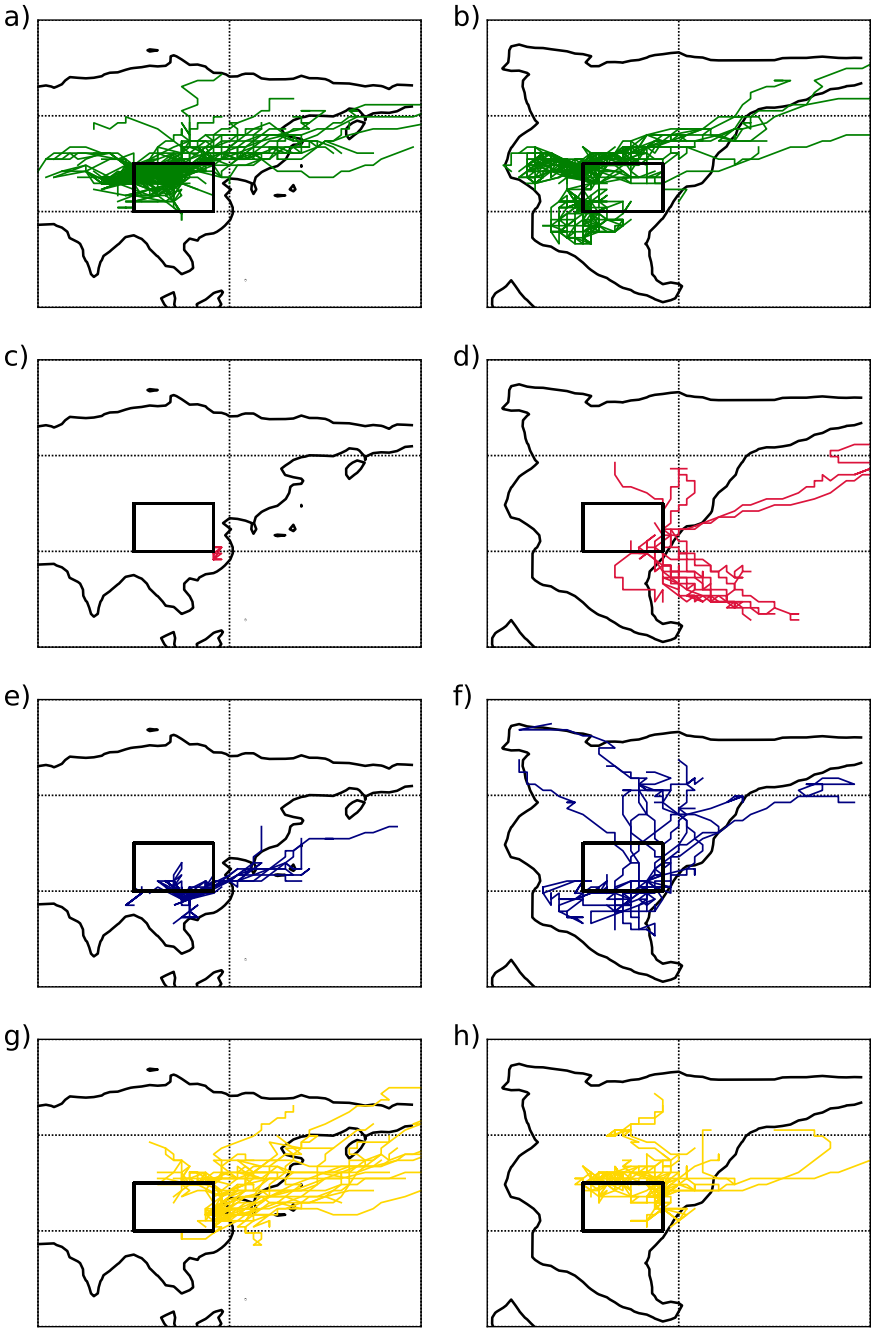


Fig. 7 Cyclone tracks crossing the focus region in July-August-Septemer, from different directions: west (a,b), southeast (c,d), south and southwest (e,f), north and northeast (g,h). The first column is from the pre-industrial control simulation and the second column is from the early Eocene ($6xCO_2$) simulation

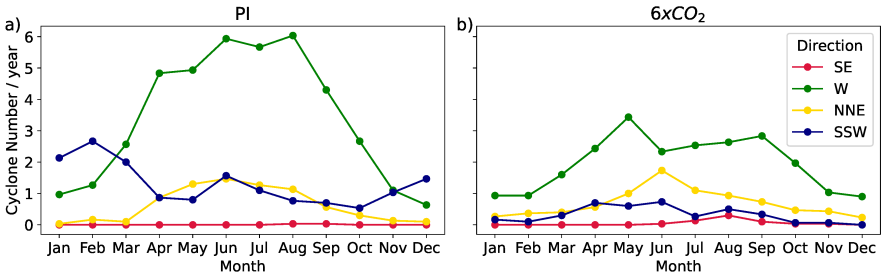


Fig. 8 The monthly distribution of the cyclones crossing the focus region from four directions (SE: southeast, W: west, NNE: north and northeast, SSW: south and southwest) in the pre-industial (a) and in the early Eocene ($6xCO_2$) simulation (b)

References

Abhik S, Capitanio FA, Goswami B, et al (2026) A brief history of asian summer monsoon evolution in the cenozoic era. npj Climate and Atmospheric Science 9(1):5. https://doi.org/10.1038/s41612-025-01259-7

Bondarenko OV, Utescher T (2026) A homogeneous green belt: zonal vegetation of east asia in the eocene. Botanica Pacifica 15(1):3–21. https://doi.org/10.17581/bp.2026.15108

Chen J, Bordoni S (2014) Orographic effects of the tibetan plateau on the east asian summer monsoon: An energetic perspective. Journal of Climate 27(8):3052–3072. https://doi.org/10.1175/JCLI-D-13-00479.1

Farnsworth A, Lunt DJ, Robinson SA, et al (2019) Past east asian monsoon evolution controlled by paleogeography, not co2. Science Advances 5(10):eaax1697. https://doi.org/10.1126/sciadv.aax1697

Farnsworth A, Lunt D, Valdes P, et al (2026) What were the role of palaeogeography in east asian monsoon evolution since the cretaceous? National Science Review p nwag534. https://doi.org/10.1093/nsr/nwag534/8785785

Geen R, Bordoni S, Battisti DS, et al (2020) Monsoons, itczs, and the concept of the global monsoon. Reviews of Geophysics 58(4):e2020RG000700. https://doi.org/10.1029/2020RG000700

Grimm GW, Denk T (2012) Reliability and resolution of the coexistence approach—a revalidation using modern-day data. Review of Palaeobotany and Palynology 172:33–47. https://doi.org/10.1016/j.revpalbo.2012.01.006

Grimm GW, Potts AJ (2016) Fallacies and fantasies: the theoretical underpinnings of the coexistence approach for palaeoclimate reconstruction. Climate of the Past 12(3):611–622. https://doi.org/10.5194/cp-12-611-2016, URL https://cp.copernicus.org/articles/12/611/2016/

Grimm GW, Bouchal JM, Denk T, et al (2016) Fables and foibles: A critical analysis of the palaeoflora database and the coexistence approach for palaeoclimate reconstruction. Review of Palaeobotany and Palynology 233:216–235. https://doi.org/10.1016/j.revpalbo.2016.07.001

Guo Z, Sun B, Zhang Z, et al (2008) A major reorganization of asian climate by the early miocene. Climate of the Past 4(3):153–174. https://doi.org/10.5194/cp-4-153-2008

Ha KJ, Heo KY, Lee SS, et al (2012) Variability in the east asian monsoon: A review. Meteorological Applications 19(2):200–215. https://doi.org/10.1002/met.1320

He Z, Zhang Z, Guo Z, et al (2025) The origin of the modern-like east asian monsoon: insights from new proxy data synthesis and climate modelling. Earth-Science Reviews p 105297. https://doi.org/10.1016/j.earscirev.2025.105297

Hollis CJ, Dunkley Jones T, Anagnostou E, et al (2019) The deepmip contribution to pmip4: Methodologies for selection, compilation and analysis of latest paleocene and early eocene climate proxy data, incorporating version 0.1 of the deepmip database. Geoscientific Model Development 12(7):3149–3206. https://doi.org/10.5194/gmd-12-3149-2019

Hu Y, Li X, Boos WR, et al (2023) Emergence of the modern global monsoon from the pangaea megamonsoon set by palaeogeography. Nature Geoscience 16(11):1041–1046. https://doi.org/10.1038/s41561-023-01288-y

Hönisch B, Royer DL, Breecker DO, et al (2023) Toward a cenozoic history of atmospheric co¡sub¿2¡/sub¿. Science 382(6675):eadi5177. https://doi.org/10.1126/science.adi5177, URL https://www.science.org/doi/abs/10.1126/science.adi5177, https://www.science.org/doi/pdf/10.1126/science.adi5177

IPCC (2021) Annex v: Monsoons. In: Masson-Delmotte V, Zhai P, Pirani A, et al (eds) Climate Change 2021: The Physical Science Basis. Contribution of Working Group I to the Sixth Assessment Report of the Intergovernmental Panel on Climate Change. Cambridge University Press, Cambridge, United Kingdom and New York, NY, USA, chap Annex V: Monsoons, p 2193–2204, https://doi.org/10.1017/9781009157896.019

Kaya MY, Dupont-Nivet G, Proust JN, et al (2019) Paleogene evolution and demise of the proto-paratethys sea in central asia (tarim and tajik basins): Role of intensified tectonic activity at ca. 41 ma. Basin Research 31(3):461–486. https://doi.org/10.1111/bre.12330

Kelemen FD (2025) Cesm1.2 simulation data for the paper "role of paleogeography on large-scale circulation during the early eocene". https://doi.org/10.5281/zenodo.17246902, URL https://doi.org/10.5281/zenodo.17246902

Kelemen FD (2026) Cesm1.2 simulation data for the paper "the east asian summer monsoon and tropical cyclones shape mid-latitude precipitation in the early eocene hothouse climate". https://doi.org/10.5281/zenodo.22302765, URL https://doi.org/10.5281/zenodo.22302765

Kelemen FD, Bartholy J, Pongracz R (2015) Multivariable cyclone analysis in the mediterranean region. Időjárás 119(2):159–184

Kelemen FD, Steinig S, de Boer A, et al (2023) Meridional heat transport in the deepmip eocene ensemble: Non-co2 and co2 effects. Paleoceanography and Paleoclimatology 38(8):e2022PA004607. https://doi.org/10.1029/2022PA004607

Kelemen FD, Lohmann R, Zhu J, et al (2026) Role of paleogeography on large-scale circulation during the early eocene. Climate of the Past 22(3):505–516. https://doi.org/10.5194/cp-22-505-2026

Li XJ, Zhu BQ (2024) Interaction between the westerlies and asian monsoons in the middle latitudes of china: Review and prospect. Atmosphere 15(3):274. https://doi.org/10.3390/atmos15030274

Licht A, Van Cappelle M, Abels HA, et al (2014) Asian monsoons in a late eocene greenhouse world. Nature 513(7519):501–506. https://doi.org/10.1038/nature13704

Lunt DJ, Huber M, Anagnostou E, et al (2017) The deepmip contribution to pmip4: Experimental design for model simulations of the eeco, petm, and pre-petm (version 1.0). Geoscientific Model Development 10(2):889–901. https://doi.org/10.5194/gmd-10-889-2017

Lunt DJ, Bragg F, Chan WL, et al (2021) Deepmip: Model intercomparison of early eocene climatic optimum (eeco) large-scale climate features and comparison with proxy data. Climate of the Past 17:203–227. https://doi.org/10.5194/cp-17-203-2021

Ma Z, Cheng L, Camargo SJ, et al (2026) Interactions of tropical cyclones with global energy and water cycles. Nature Reviews Earth & Environment pp 1–19. https://doi.org/10.1038/s43017-026-00770-6

McInerney FA, Wing SL (2011) The paleocene-eocene thermal maximum: A perturbation of carbon cycle, climate, and biosphere with implications for the future. Annual Review of Earth and Planetary Sciences 39(1):489–516. https://doi.org/10.1146/annurev-earth-040610-133431

Meijer N, Dupont-Nivet G, Abels HA, et al (2019) Central asian moisture modulated by proto-paratethys sea incursions since the early eocene. Earth and Planetary Science Letters 510:73–84. https://doi.org/10.1016/j.epsl.2018.12.031

Meijer N, Licht A, Woutersen A, et al (2024) Proto-monsoon rainfall and greening in central asia due to extreme early eocene warmth. Nature Geoscience 17(2):158–164. https://doi.org/10.1038/s41561-023-01371-4

Quan C, Liu YSC, Utescher T (2012a) Eocene monsoon prevalence over china: A paleobotanical perspective. Palaeogeography, Palaeoclimatology, Palaeoecology 365-366:302–311. https://doi.org/https://doi.org/10.1016/j.palaeo.2012.09.035, URL https://www.sciencedirect.com/science/article/pii/S0031018212005482

Quan C, Liu YSC, Utescher T (2012b) Paleogene temperature gradient, seasonal variation and climate evolution of northeast china. Palaeogeography, Palaeoclimatology, Palaeoecology 313-314:150–161. https://doi.org/https://doi.org/10.1016/j.palaeo.2011.10.016, URL https://www.sciencedirect.com/science/article/

pii/S0031018211005256

Roe GH, Ding Q, Battisti DS, et al (2016) A modeling study of the response of asian summertime climate to the largest geologic forcings of the past 50 ma. JournalofGeophysicalResearch: Atmospheres 121(10):5453r5470. https://doi.org/10.1002/2015JD024370

Son JH, Seo KH, Wang B (2019) Dynamical control of the tibetan plateau on the east asian summer monsoon. Geophysical Research Letters 46(13):7672–7679. https://doi.org/10.1029/2019GL083104

Spicer RA, Farnsworth A, Su T, et al (2025) The progressive co-evolutionary development of the pan-tibetan highlands, the asian monsoon system and asian biodiversity https://doi.org/doi.org/10.1144/SP549-2023-180

Stein RA, Sheldon ND, Smith SY (2021) Soil carbon isotope values and paleoprecipitation reconstruction. Paleoceanography and Paleoclimatology 36(4):e2020PA004158. https://doi.org/10.1029/2020PA004158

Su LF, Zhang QQ, Sun YK, et al (2022) New evidence of the emergence of the east asian monsoon in the early palaeogene. Scientific Reports 12(1):20471. https://doi.org/10.1038/s41598-022-24298-z

Sun X, Wang P (2005) How old is the asian monsoon system?—palaeobotanical records from china. Palaeogeography, Palaeoclimatology, Palaeoecology 222(3):181–222. https://doi.org/https://doi.org/10.1016/j.palaeo.2005.03.005, URL https://www.sciencedirect.com/science/article/pii/S0031018205001203

Tardif D, Fluteau F, Donnadieu Y, et al (2020) The origin of asian monsoons: A modelling perspective. Climate of the Past 16(3):847–865. https://doi.org/10.5194/cp-16-847-2020

Tardif D, Sarr AC, Fluteau F, et al (2023) The role of paleogeography in asian monsoon evolution: a review and new insights from climate modelling. Earth-Science Reviews 243:104464. https://doi.org/10.1016/j.earscirev.2023.104464

Thompson N, Salzmann U, Hutchinson DK, et al (2025) Global vegetation zonation and terrestrial climate of the warm early eocene. Earth-Science Reviews 261:105036. https://doi.org/10.1016/j.earscirev.2024.105036

Tierney JE, Zhu J, Li M, et al (2022) Spatial patterns of climate change across the paleocene–eocene thermal maximum. Proceedings of the national academy of sciences 119(42):e2205326119. https://doi.org/10.1073/pnas.2205326119

Utescher T, Bruch A, Erdei B, et al (2014) The coexistence approach—theoretical background and practical considerations of using plant fossils for climate quantification. Palaeogeography, Palaeoclimatology, Palaeoecology 410:58–73. https://doi.

org/10.1016/j.palaeo.2014.05.031

Wang B, Ding Q (2008) Global monsoon: Dominant mode of annual variation in the tropics. Dynamics of Atmospheres and Oceans 44(3-4):165–183. https://doi.org/10.1016/j.dynatmoce.2007.05.002

Wang B, Jin C, Liu J (2020) Understanding future change of global monsoons projected by cmip6 models. Journal of Climate 33(15):6471–6489. https://doi.org/10.1175/JCLI-D-19-0993.1

Wang Q, Ferguson DK, Feng GP, et al (2010) Climatic change during the palaeocene to eocene based on fossil plants from fushun, china. Palaeogeography, Palaeoclimatology, Palaeoecology 295(1-2):323–331

Westerhold T, Marwan N, Drury AJ, et al (2020) An astronomically dated record of earth's climate and its predictability over the last 66 million years. Science 369(6509):1383–1387. https://doi.org/10.1126/science.aba6853, URL https://www.science.org/doi/abs/10.1126/science.aba6853

Wynn JG (2007) Carbon isotope fractionation during decomposition of organic matter in soils and paleosols: Implications for paleoecological interpretations of paleosols. Palaeogeography, Palaeoclimatology, Palaeoecology 251(3-4):437–448. https://doi.org/10.1016/j.palaeo.2007.04.009

Xie Y, Wu F, Fang X (2022a) Abrupt collapse of a swamp ecosystem in northeast china during the paleocene–eocene thermal maximum. Palaeogeography, Palaeoclimatology, Palaeoecology 595:110975. https://doi.org/https://doi.org/10.1016/j.palaeo.2022.110975, URL https://www.sciencedirect.com/science/article/pii/S0031018222001456

Xie Y, Wu F, Fang X (2022b) A transient south subtropical forest ecosystem in central china driven by rapid global warming during the paleocene-eocene thermal maximum. Gondwana Research 101:192–202. https://doi.org/https://doi.org/10.1016/j.gr.2021.08.005, URL https://www.sciencedirect.com/science/article/pii/S1342937X21002471

Xie Y, Wu F, Wang H, et al (2024) Onset of aridification in mid-latitude asia at 41 ma linked to the proto-paratethys sea retreat. Gondwana Research 131:196–207. https://doi.org/https://doi.org/10.1016/j.gr.2024.03.007, URL https://www.sciencedirect.com/science/article/pii/S1342937X24000650

Xie Y, Wu F, Miao Y, et al (2025) Reappraisal of eocene climate patterns in east asia: A synthetic review. Earth-Science Reviews p 105281. https://doi.org/10.1016/j.earscirev.2025.105281

Yao YF, Bera S, Ferguson DK, et al (2009) Reconstruction of paleovegetation and paleoclimate in the early and middle eocene, hainan island, china. Climatic Change

92(1):169–189. https://doi.org/10.1007/s10584-008-9457-2

Zhang QQ, Smith T, Yang J, et al (2016) Evidence of a cooler continental climate in east china during the warm early cenozoic. PLoS One 11(5):e0155507. https://doi.org/10.1371/journal.pone.0155507

Zhang Z, Flatøy F, Wang H, et al (2012) Early eocene asian climate dominated by desert and steppe with limited monsoons. Journal of Asian Earth Sciences 44:24–35. https://doi.org/10.1016/j.jseaes.2011.05.013

Zhu J, Poulsen CJ, Tierney JE (2019) Simulation of eocene extreme warmth and high climate sensitivity through cloud feedbacks. Science advances 5(9):eaax1874. https://doi.org/10.1126/sciadv.aax1874

Zhu J, Poulsen CJ, Tierney JE (2024) Cesm1.2 simulation data for "simulation of eocene extreme warmth and high climate sensitivity through cloud feedbacks". https://doi.org/10.5281/zenodo.12702135, URL https://doi.org/10.5281/zenodo.12702135

Declarations

Funding

This research was supported by the EarthCriSys (Earth System Critical Thresholds) project by the Rhineland-Palatinate Research Initiative. This work used resources of the Deutsches Klimarechenzentrum (DKRZ) granted by its Scientific Steering Committee (WLA) under project ID1346. The CESM project is supported primarily by the National Science Foundation (NSF). This material is based upon work supported by the National Center for Atmospheric Research (NCAR), which is a major facility sponsored by the NSF under Cooperative Agreement No. 1852977.

Competing Interests

The authors have no conflicts of interest to declare that are relevant to the content of this article.

Author Contributions

Both authors contributed to the study conception and design. Data collection was performed by Niels Meijer and the simulations were performed by Fanni Dóra Kelemen. Analysis was performed by Fanni Dóra Kelemen. The first draft of the manuscript was written by Fanni Dóra Kelemen and Niels Meijer and both read and approved the final manuscript.

Data Availability

The proxy compilation consists already published records, the summary of our compilation is available in the appendix (Table A1). The DeepMIP CESM1.2 simulations are available by following the instructions at https://www.deepmip.org/data-eocene/ and the restart files at Zhu et al. (2024). The atmosphere-only simulations used for this study are available at Kelemen (2026, 2025).